Experimental and theoretical studies of the effect of molecular conformation on the photophysical properties in the pyrene system

Xinyi Song,[a] Hongxi Guo,[a] Shuning Yu,[a] Carl Redshaw,[b] Qilong Zhang,[c] Ruquan Ye,[d] Xing Feng*[a,e]

[a] Guangdong Provincial Key Laboratory of Information Photonics Technology, School of Material and Energy, Guangdong University of Technology, Guangzhou 510006, P. R. China. E-mail: hyxhn@sina.com (X. Feng)

[b] Department of Chemistry, University of Hull, Cottingham Road, Hull, Yorkshire HU6 7RX, U.K.

[c] School of Public Health, The Key Laboratory of Environmental Pollution, Monitoring and Disease Control, Ministry of Education, Guizhou Medical University, Guiyang 550025, China

[d] Department if chemistry, state key laboratory of marine pollution, City university of Hong Kong, Kowloon Tong, Hong Kong 999077, China.

[e] Guangdong Provincial Key Laboratory of Luminescence from Molecular Aggregates (South China University of Technology) Guangzhou 510640, China

Abstract: Disordered motion is an intrinsic property of molecules. The use of controllable molecular motion can not only achieve interesting molecular geometry, but can also induce novel opto-electronic behaviour. Herein, a set of pyrene-based compounds were synthesized to realize an observable molecular motion. 2,5-Dimethoxyphenyl unit (s) were introduced at the pyrene core, which lead to different molecular conformations. Furthermore, the detail molecular geometries of the compounds were investigated by NMR spectroscopy and DFT calculations. In addition, the photophysical properties of these compounds were investigated in order to understand the relationship between the molecular conformations and the photophysical properties. The diversiform of molecular conformations can cause a broaden FWHM emission in organic luminescence materials.

Keywords: Pyrene, blue emitter, molecular conformation, molecular rotation, structure-properties relationship

Introduction

Organic luminescent materials have attracted great attention over the past decades, due to their significant application in opto-electronic devices,[1],[2] super-resolution imaging,[3],[4] and anti-counterfeiting.[5],[6] The optical properties of organic luminescent materials are not only closely related to their molecular structure, packing mode and morphology, but also the molecular conformation can play a significant role in affecting the electronic coupling.[7],[8] The synergistic effect of the above-mentioned factors can result in fantastic optical, electrical, and magnetic behaviour for organic luminescent materials. For example, mechanochromic and mechanoluminescence materials exhibit tuneable emission colour properties under mechanical stimulus due to changes in their molecular assemblies.[9],[10],[11] Yu *et al*. reported that photoresponsive tristable chiral cholesteric liquid crystals (CLCs) can be subject to piecewise control of the reflection wavelength from the visible spectrum to the near-infrared region upon irradiation, which is related to the molecular conformation change on going from (*trans*, *trans*, *trans*, *trans*) to (*cis*, *cis*, *cis*, *cis*). [12]

Moreover, molecular motion/rotation is a type of ubiquitous and spontaneous behaviour.[13],[14] Disordered molecular motion can lead to various molecular conformations, and is mainly dominated by the microenvironment (such as light, temperature, solvent, etc.) and inter/intramolecular interactions (hydrogen bond, van der Waals force and π-π stacking).[15],[16],[17] When the spontaneous molecular motion/rotation is restricted by weak inter/intramolecular interactions, then the emission can be quenched or enhanced depending on the chemical structure of the luminescent molecules.[18],[19] For example, traditional fluorophores with large planar structures (such as pyrene, anthracence) can emit bright emission in dilute solution, but would exhibit weakened fluorescence in the aggregation state with a relative low quantum yield *via* strong π-π stacking interactions. Meanwhile, the sterically congested compounds with a twist conformation, like tetraphenylethylene, silole, as well as

cyanostyrene and its derivatives, display the opposite optical behaviour,[18] and exhibit weak emission in solution but bright emission in the aggregation state.[20] This phenomenon was defined as aggregation-induced emission by Tang and co-workers in 2001,[21] and is due to the restriction of the free rotation/motion of the molecule by intermolecular interactions, *i.e.* the non-radiative decay pathway has been blocked and the excitation energy populates the radiative decay pathway.[22]

In fact, it is that the molecule rotation lead to various molecular conformations, involving molecular stereo conformation, *cis-tran* isomerism and chirality, etc., and this was accompanied by distinguishable properties.[23] This is important fundamental research in the field of structural chemistry. Generally, the subtle difference of molecular conformation can be identified by NMR spectroscopic coupling constants, by single crystal X-ray diffraction analysis, as well as by theoretical calculations.

Pyrene is a four phenyl-fused polycyclic aromatic hydrocarbons compound with a rigid planar structure, which displays an intense deep blue emission with a high quantum yield in solution, but prefers to form a dimer *via* π-π stacking, leading to quenched fluorescence.[24],[25] Bulky substituent group(s) have been introduced at the pyrene core, which can not only inhibit the π-π stacking, but also produce different emission behaviour. For example, the compound 1-(4-(phenylsulfonyl)phenyl)pyrene adopts two types of crystal pattern model exhibiting sky-blue and green excimer fluorescence, due to different single-molecule conformations.[26] On the other hand, Lee *et al*. observed that 1,6-di(pyridin-3-yl)-3,8-di(naphthalen-1-yl)pyrene (N1PP) displayed a small bandgap, and a more blue-shifted emission compared to 1,6-di(pyridin-3-yl)-3,8-di(naphthalen-2-yl)pyrene (N2PP), whilst the later exhibited great electroluminescence properties.[27] Although it is popular to explore the molecular structure-properties relationship for various application,[28] few examples focus on investigating the effect of the molecular conformation for the optical behaviour in pyrene chemistry. In this article, we present a series of pyrene-based blue emitters with the 2,5-dimethoxyphenyl unit at the 1-, 3-, 6- and 8-positions and investigate the resulting photophysical properties. Due to the differing molecular rotation around the C-C bond, these compounds display different molecular conformations and optical

behaviour.

Experimental section

Materials

Unless otherwise stated, all reagents used were purchased from commercial sources and were used without further purification. Tetrahydrofuran was distilled prior to use. The 1-bromopyrene,[29] 1,3-dibromopyrene,[30] and 1,3,6,8-tetrabromopyrene[28], [31] were synthesized following the literature.

Characterization

$^{1}H/^{13}C$ NMR spectra were recorded on a Bruker AV 400M spectrometer using chloroform-*d* solvent and tetramethylsilane as internal reference. *J*-values are given in Hz. High-resolution mass spectra (HRMS) were recorded on a LC/MS/MS, which consisted of a HPLC system (Ultimate 3000 RSLC, Thermo Scientific, USA) and a Q Exactive Orbitrap mass spectrometer. UV-vis absorption spectra and photoluminescence (PL) spectra were recorded on a Shimadzu UV-2600 and the Hitachi F-4700 spectrofluorometer. PL quantum yields were measured using absolute methods using a Hamamatsu C11347-11 Quantaurus-QY Analyzer. The lifetime was recorded on an Edinburgh FLS 980 instrument and measured using a time-correlated single-photon counting method. Thermogravimetric analysis was carried on a Mettler Toledo TGA/DSC3+ under dry nitrogen at a heating rate of 10 ºC/min. The quantum chemistry calculations were performed using the Gaussian 09 (B3LYP/6–311G (d,p) basis set) software package.

X-ray Crystallography.

Crystallographic data for **1** was collected on a Bruker APEX 2 CCD diffractometer with graphite monochromated Mo Kα radiation (λ = 0.71073 Å) in the ω scan mode.[32] The structure was solved by charge flipping algorithms and refined by full-matrix least-squares methods on F^2.[33],[34] All esds (except the esd in the dihedral angle between two l.s. planes) were estimated using the full covariance matrix. The cell esds were considered individually in the estimation of esds in distances, angles and torsion angles. Correlations between esds in cell parameters were only used when they were defined by crystal symmetry. An approximate (isotropic) treatment of cell esds was used for

estimating esds involving l.s. planes. The final cell constants were determined through global refinement of the xyz centroids of the reflections harvested from the entire data set. Structure solution and refinements were carried out using the SHELXTL-PLUS software package.[33] Data (excluding structure factors) on the structure reported here has been deposited with the Cambridge Crystallographic Data Centre. CCDC 2184638 for **2b** contains the supplementary crystallographic data for this paper. These data could be obtained free of charge from The Cambridge Crystallographic Data Centre via www.ccdc.cam.ac.uk/data_request/cif.

General procedure for the synthesis of compounds 1-4

The compounds **1-4** were synthesized from (2,5-dimethoxyphenyl)boronic acid using different bromopyrene intermediates by a Suzuki coupling reaction in high yield.

Synthesis of 7-*tert*-butyl-1-(2,5-dimethoxyphenyl)pyrene (1)

Under a nitrogen atmosphere, to a stirred solution of 1-bromo-7-*tert*-butyl pyrene (400 mg, 1.17 1 eq.) in toluene (12 mL), ethanol (2 mL) and water (2 mL), was added K_2CO_3 (400 mg, 2.89 mmol) and (2,5-dimethoxyphenyl)boronic acid (260 mg, 1.43 mmol, 1.2 eq.). The mixture was stirred for 5 min and then tetrakis(triphenylphosphine)palladium ($Pd(PPh_3)_4$) (100 mg, 0.09 mmol) was added, and the dark suspension was heated to 90 ℃ with stirring for 24 h. After cooling, the mixture was quenched by H_2O (50 mL) and extracted by CH_2Cl_2 (50 mL× 3) three times, and the organic layer was washed successively washed with water and brine. The combined organic extracts were dried with anhydrous $MgSO_4$ and then evaporated. The residue was purified by column chromatography eluting with CH_2Cl_2-hexane (4:1) to give 7-*tert*-butyl-1-(2,5-dimethoxyphenyl)pyrene (**1**) as a white powder. Recrystallisation from a mixture of CH_2Cl_2 and hexane afforded the target compound **1** as white crystals (180 mg, 38 %. melting point: 128~130 ℃). ^{1}H NMR (400 MHz, $CDCl_3$) δ 8.22 (d, J = 1.8 Hz, 1H), 8.19 (d, J = 7.8 Hz, 1H), 8.19 (d, J = 1.8 Hz, 1H), 8.07 (s, 2H), 7.97 (d, J = 9.2 Hz, 1H), 7.92 (d, J = 7.8 Hz, 1H), 7.86 (d, J = 9.2 Hz, 1H), 7.09 – 6.97 (m, 3H), 3.84 (s, 3H), 3.65 (m, 3H), 1.59 (s, 9H) ppm. ^{13}C NMR (100 MHz, $CDCl_3$) δ 153.7, 151.7, 149.1, 134.0, 131.3, 131.1, 130.9, 130.6, 129.1, 127.6, 127.6, 127.4, 125.9, 124.7, 124.4, 123.2, 122.4, 122.2, 118.2, 113.7, 112.7, 56.4, 55.9, 53.5, 35.3, 32.0 ppm. HRMS (FTMS+p

APCI): m/z+H^+ calcd for $C_{28}H_{26}O_2$ 395.1966, found 395.2000 $[M+H]^+$.

7-*tert*-butyl-1,3-bis(2,5-dimethoxyphenyl)pyrene (2) was synthesized by a similar reaction to give 7-*tert*-butyl-1,3-bis(2,5-dimethoxyphenyl)pyrene as a white powder by column chromatography eluting with CH_2Cl_2-hexane (**3:1**). Recrystallisation from mixture of CH_2Cl_2 and hexane achieved the target compound **2** as a white powder (170 mg, 44 %. melting point: 122~123 ℃). ^{1}H NMR (400 MHz, $CDCl_3$) δ 8.18 (s, 2H), 7.98 (d, *J* = 9.2 Hz, 2H), 7.93-7.85 (m, 3H), 7.09 (d, *J* = 2.9 Hz, 1H), 7.07 – 6.96 (m, 5H), 3.84 (s, 3H), 3.83 (s, 3H), 3.68 (s, 3H), 3.65 (s, 3H), 1.58 (s, 9H) ppm. ^{13}C NMR (100 MHz, $CDCl_3$) δ 153.7, 153.6, 151.9, 151.7, 149.0, 148.9, 133.4, 131.2, 131.1, 131.0, 129.8, 129.7, 128.7, 128.6, 127.3, 127.2, 125.9, 125.8, 124.9, 124.8, 123.3, 123.3, 122.2, 118.3, 118.3, 113.9, 113.7, 112.9, 112.5, 56.5, 56.4, 55.9, 35.2, 32.0 ppm. HRMS (FTMS+p APCI): m/z+H^+ calcd for $C_{36}H_{34}O_4$ 531.2491, found 531.2532 $[M+H]^+$.

Synthesis of 1,3,6-tris(2,5-dimethoxyphenyl)pyrene (3) and 1,3,6,8-tetrakis(2,5-dimethoxyphenyl)pyrene (4) were purified by column chromatography eluting with CH_2Cl_2-hexane (1:2) to give 1,3,6-tris(2,5-dimethoxyphenyl)pyrene (**3**) (160 mg,45%. melting point :152~153℃) as a light yellow powder, and CH_2Cl_2-hexane (1:1) as eluate to give 1,3,6,8-tetrakis(2,5-dimethoxyphenyl)pyrene (**4**) as a yellow powder. ^{1}H NMR (400 MHz, $CDCl_3$) δ 8.19 (d, *J* = 7.8 Hz, 1H), 8.01 (d, *J* = 9.2 Hz, 1H), 7.97 – 7.89 (m, 3H), 7.88 – 7.75 (m, 2H), 7.13 – 6.92 (m, 9H), 3.88 – 3.77 (m, 9H), 3.71 – 3.56 (m, 9H) ppm. ^{13}C NMR (100 MHz, $CDCl_3$) δ 153.7, 153.6, 153.6, 151.9, 151.9, 151.9, 151.8, 151.7, 151.7, 134.1, 134.0, 134.0, 133.6, 133.6, 133.5, 133.4, 133.4, 131.4, 131.3, 131.2, 131.2, 131.1, 131.0, 130.9, 130.9, 130.1, 130.1, 130.0, 129.3, 129.1, 129.1, 128.7, 128.0, 127.9, 127.9, 127.1, 125.9, 125.9, 125.8, 125.7, 125.6, 125.6, 125.5, 125.2, 125.1, 125.1, 125.0, 124.5, 124.4, 118.3, 118.2, 118.1, 113.9, 113.8, 113.8, 113.7, 113.6, 113.0, 112.9, 112.8, 112.6, 112.5, 112.5, 112.4, 56.5, 56.5, 56.4, 56.4, 56.4, 56.3, 55.9, 55.9 ppm. HRMS (FTMS+p APCI): m/z+H^+ calcd for $C_{40}H_{34}O_6$ 611.2389, found 611.2427 $[M+H]^+$. For 1,3,6,8-tetrakis(2,5-dimethoxyphenyl)pyrene (**4**): ^{1}H NMR (400 MHz, CDCl3) δ 7.91 (dd, *J* = 6.1, 3.4 Hz, 2H), 7.84 (d, *J* = 5.9 Hz, 2H), 7.81 (d, *J* = 6.6 Hz, 2H), 7.15 – 6.89 (m, 12H), 3.82 (dd, *J* = 6.4, 2.3 Hz, 12H), 3.63 (ddd, *J* = 11.6, 7.7, 4.3 Hz, 12H) ppm. ^{13}C NMR (100 MHz, $CDCl_3$) δ 153.6, 153.6, 151.8, 151.7, 151.7, 133.4,

133.4, 133.4, 133.2, 131.3, 131.3, 131.2, 131.1, 131.0, 130.0, 129.9, 129.8, 128.9, 128.8, 128.8, 128.1, 125.6, 125.5, 125.4, 125.2, 125.1, 125.0, 118.3, 118.3, 118.2, 118.2, 118.1, 113.9, 113.8, 113.8, 113.7, 113.6, 113.6, 113.0, 112.9, 112.8, 112.8, 112.5, 112.4, 112.3, 56.5, 56.4, 56.3, 55.9, 53.5 ppm. HRMS (FTMS+p APCI): m/z+H^+ calcd for $C_{48}H_{42}O_8$ 747.2913, found 747.2950 $[M+H]^+$.

1,3,6,8-tetrakis(2,5-dimethoxyphenyl)pyrene (4) was purified by column chromatography eluting with CH_2Cl_2-hexane (3:2) to give 1,3,6,8-tetrakis(2,5-dimethoxyphenyl)pyrene (**4**) (150 mg, 35%, melting point >300 ℃) as a yellow powder.

Preparation of test solutions of compounds 1-4 for spectroscopic experiments:

The requisite amount of each pyrene-based molecule (**1-4**) was dissolved into a 10 mL volumetric flask, using THF (spectroscopic pure) as solvent, and the mother solution (10^{-3} mol/L) was prepared for later use.

Solvent effect measurements:

Taking 30 μL of each sample of mother solution into a 3 mL volumetric flask and diluting to volume with solvent (such as cyclohexane (Cy), tetrahydrofuran (THF), 1,4-dioxane (1,4-dioxane), *N*,*N*-dimethylformamide (DMF)), acetonitrile (ACN) and dimethyl sulfoxide (DMSO)), respectively, the test samples with concentration of 1×10-5 mol/L were prepared for later use.

Viscosity-dependent PL experiments:

The requisite amount of each pyrene-based molecule (**1-4**) was dissolved into a 10 mL volumetric flask, using DMSO (spectroscopic pure) as solvent for preparing a concentration of 1×10^{-3} mol/L for later use. The test samples were prepared by adding 30 μL of each sample into different proportions ratios of DMSO and glycerol solution such as glycerol solution:DMSO = 0, 1:9, 2:8, 3:7; 4:6, 5:5, 6:4, 7:3, 8:2, 9:1, respectively.

Results and discussion

Synthesis and characterization

The pyrene-based molecules **1-4** are presented in Figure 1, and were synthesized by the Suzuki-Miyaura cross-coupling reaction between (2,5-

dimethoxyphenyl)boronic acid and the corresponding bromopyrene intermediates in high yield (Scheme 1).[28], [29] All molecular structures were characterized by $^{1}H/^{13}C$ NMR spectra and high-resolution mass spectrometry (HRMS). As the number of substituent groups increases, the solubility slightly decreases in common organic solvents, such as cyclohexane (Cy), tetrahydrofuran (THF), chloroform ($CHCl_3$), *N*,*N*-dimethylformamide (DMF), and dimethyl sulfoxide (DMSO).

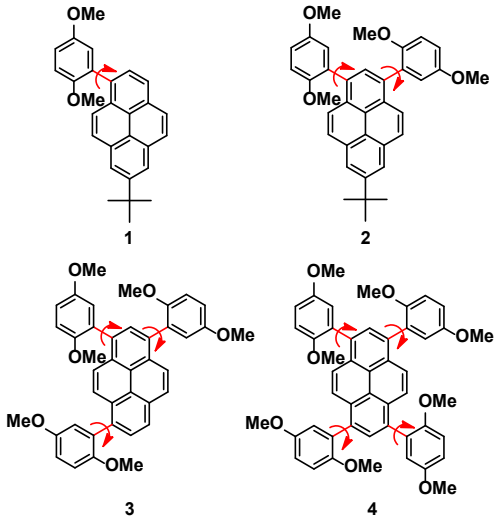

Scheme 1 The molecular structures of pyrene-derivatives **1-4.**

Thermal stability

The thermal stability of the compounds **1-4** was investigated by thermogravimetric analysis (TGA), and their thermal data are summarized in Table 1. As shown in Figure S20, the compounds exhibit good thermal stability, and as the number of substituents increases, the decomposition temperatures are improved from 304 ℃ (**1**) to 434 ℃ (**4**) (5% weight loss). The carbonized residue (char yield) also increased from 1.4% to 58% following the order of **4** > **3** > **2** > **1**, which may be ascribed to the higher aromatic content.[35] In addition, when the temperature is less than 200 ℃, compounds **2** and **3** still exhibit about 4.5% weight loss, which may be ascribed to the loss of the captured solvent molecules.

Single Crystal X-ray Diffraction analysis

We attempted to cultivate single crystals of **1**-**4** in different solvents, however only **1** afforded crystals suitable for X-ray crystallographic analysis. The crystals were obtained by slow evaporation of a mixture CH_2Cl_2 and hexane (V/V = 3:1) at room temperature, whereas the other three samples only formed light-yellow powders. Crystal **1** crystallizes in an orthorhombic system with space group of *P* b c a. In the asymmetric unit, the substituent group 1,4-dimethoxylphenyl group is connected to the pyrene ring which is arranged with a twisted angle of 65.6° along C10-C9 (Figure 1). Along the *a*-axis, the molecules present face-to-face slip-stacking with the centroid-to-centroid distance of 7.092 Å. Due to the presence of steric hindrance of the 1,4-dimethoxyl phenyl group and bulky *tert*-butyl group, there is no π-π stacking observed, but instead several C-H···π interactions are present (Figures S21, S22).[36]

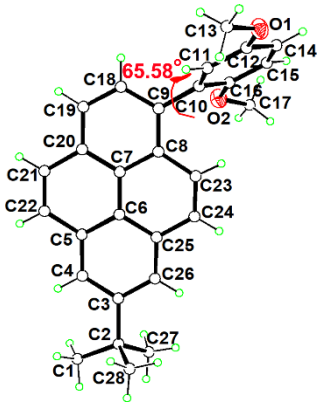

Figure 1. The X-ray structure of compound **1**.

DFT calculations

Based on our geometrical knowledge, the possible molecular conformers are summarized in Scheme 2, S1 and S2, and the electronic energies of each conformation of the pyrene derivatives were carried out by DFT calculations at the B3LYP 6-311 (d,p) level in the gas phase. Taking compound **1** as an example, the potential-energy surface of the molecular conformation **1a** shows a relatively low energy gap compared to **1b**. Moreover, the energy barrier (⊿E) of the two conformers is less than 1.57 kal/mol, suggesting that the two conformers **1a** and **1b** can interchange via free molecular rotation (Scheme 2A). Obviously, the conformer **1b** is consistent with the crystal

structure at room temperature, indicated that this is a kinetic product, and the conformer **1b** is the thermodynamic product. Similarly, molecule **2** may possess three molecular conformations with a small the energy barrier (ΔE) for each molecular conformation ($\leq$ 1.54 kal/mol), and the calculated potential-energy surface of the molecular conformations follows the order **2c** > **2b** > **2a**. Similarly, the possible molecular conformations of compounds **3** and **4** are summarized in Schemes S1 and S2, and the maximum potential-energy gap is 2.51 kal/mol for **3** and 2.61 kal/mol for **4**, respectively. Thus, the small energy barrier (ΔE) in each molecule could lead to various conformers in the same system via a molecular rotation. Furthermore, a rigid potential energy surface scan was performed by varying the torsion angle (α) from 0 to 360^{o} in the ground state and is exhibited in Figure S30 using compound **1** as example (compounds **2**, **3** and **4** have a number of different molecular conformations), the minimum energy corresponds with the conformation **1a**, and the dihedral angle between the pyrene the phenyl ring is 22.45^{o}. The conformation of **1a** changed to conformation **1b** with an enhanced potential energy as the single C-C bond rotates. This result is consistent with the experimental study. On the other hand, the optimized geometry structure of compounds **1**-**4** are summarized in Figure S29. The HOMO and LUMO orbitals of all compounds **1**-**4** have slight differences. The HOMO level of compound **1** was delocalized over the pyrene core and the substituent phenyl group, while the LUMO was mainly distributed over the pyrene ring and a fragment of the phenyl ring. As the number of substituents increased, both HOMO and LUMO levels of compounds **1**-**4** are centered over the whole pyrene core. Moreover, as the number of substituent groups increases, the energy gap decreased from 3.69 to 3.55 eV.

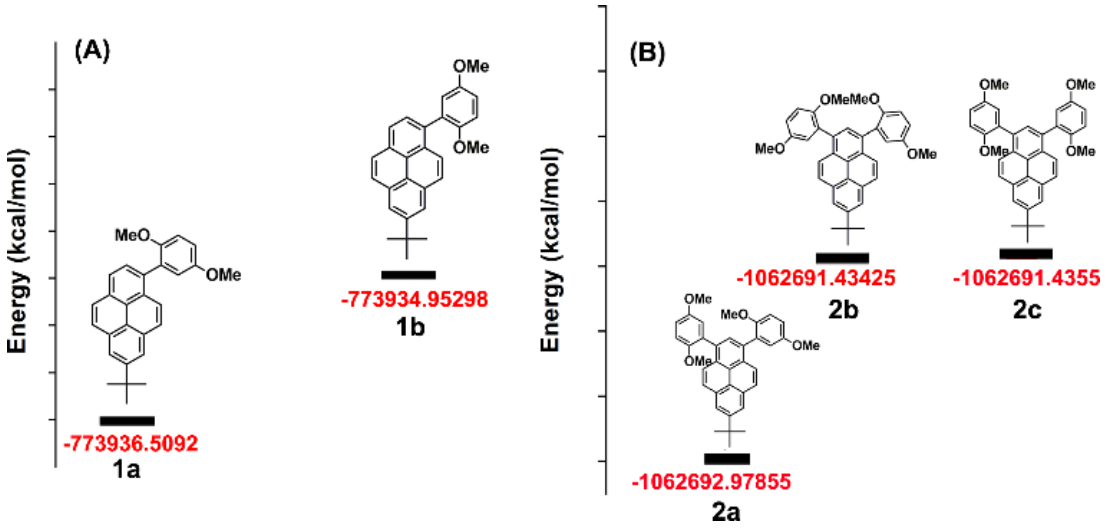

Scheme 2. Potential energy surface for **1** and **2** (Gaussian 09W (B3LYP/6-311G(d,p) basis set)).

NMR spectroscopic analysis

The ^{1}H NMR spectra of compounds **1**-**4** were performed in $CDCl_3$ at room temperature (Figure 2). For compound **1**, the proton peaks at 8.22 ppm, 8.19 ppm, 8.19 ppm, 7.97 ppm, 7.92 ppm and 7.86 ppm originate from the pyrene unit, while the proton peaks for the two methoxy groups (OMe) are at 3.65 ppm and 3.64 ppm with integral ratio of 1:1; the proton signals in the region 6.99-7.08 ppm for the phenyl ring are complicated. The integral ratio of the peaks corresponds to the formula of compound **1**. It is noteworthy that the ^{1}H NMR spectra of compounds **2**-**4** indicate that the proton peaks for the pyrene ring, the phenyl and the methoxy group (OMe) become more indistinguishable as the number of OMe groups increases. In particular, the proton signals for the pyrene and phenyl rings became unresolved and the single proton peak for the two methoxy groups splits into multiple peaks as the number of substituent groups increases, and the previous singlet identified as the carbon peak single for OMe in region of 53.5-56.4 ppm also became more complicated (Figures S2, S4, S6 and S8). It seems that compounds **1**-**4** are mixtures, but the TLC and HRMS results indicated that each compound is pure (Figure S15-S19). Thus, we infer that the OMe group experiences different chemical environments, and a different chemical shift was found in the ^{1}H/^{13}C NMR spectra. The experimental results indicated that OMe group at the 1-, 3-, 6- and 8- positions of pyrene can rotate leading to various molecular conformations, which is consistent with the DFT calculations. We assumed that each proton peak at around 3.84 and 3.64 ppm corresponds to a OMe group in a particular chemical environment. According to the ^{1}H NMR spectra of compounds **1**-**4**, there is at least one conformation for **1**, two conformations for compound **2** with mole ratio of 2:3 (integral ratio), seven conformations for compound **3** and five conformations for compound **4**, respectively. The ^{1}H NMR spectral results are similar to the mathematical modelling of the molecular conformations (compounds **1**-**4** have two, three, eight and seven, respectively).

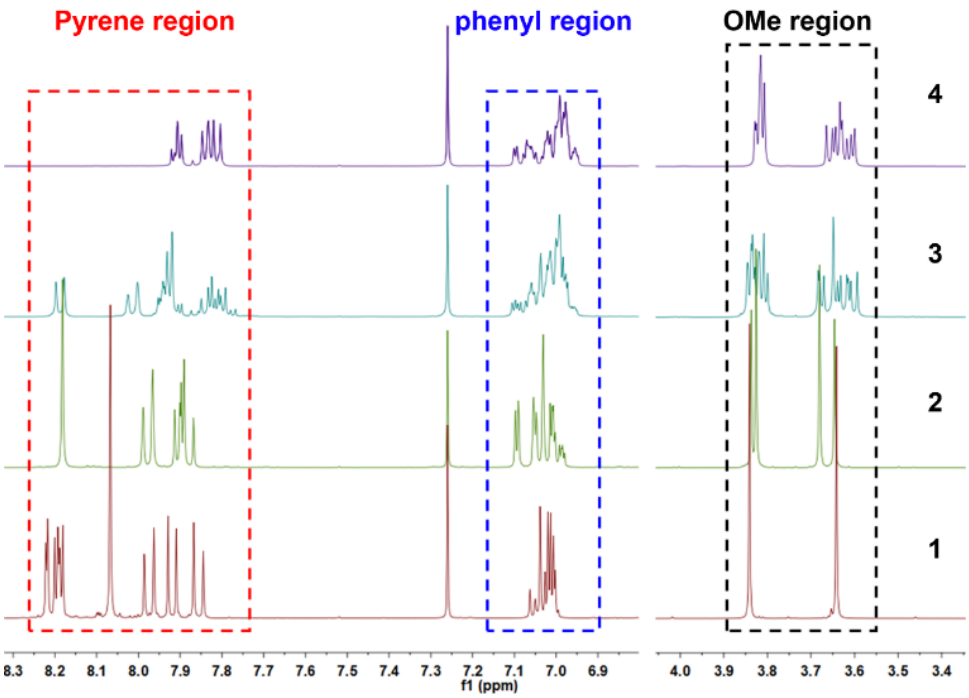

Figure 2. ^{1}H NMR spectrum (400 MHz, 293 K, * $CDCl_3$) of pyrene derivatives **1**-**4**.

The variable-temperature ^{1}H NMR spectra of compounds **1**-**4** were measured in THF-d8 in order to understand the molecular rotation around the C-C bond. As shown in Figure 3, the chemical shift of the protons at the pyrene ring and phenyl ring in **1** were shifted upfield as the temperature was increased from -50 ºC to 25 ºC (room temperature). For example, the signals at 8.36 and 8.38 ppm were shifted upfield to 8.28 and 8.31 ppm respectively, which corresponds to the protons at the 6- and 8-positions of pyrene. On the other hand, the proton peaks for the OMe group appear at 3.61, 3.65 and 3.83 ppm with the integral ratio of 1:1:1 at -50 ºC, indicated that the compound adopts conformation (**1a)** at low temperature, while the peak at 3.65 ppm was shifted upfield to 3.63 ppm and overlapped with the solvent proton peak (DMSO-d6) with integral ratio of 1:3 as the temperature rose to 25 ºC (Figure S9), indicated that the mole ratio conformation **1a** and **1b** is 1:1. In addition, the proton integration ratio for the OMe group changed to 1:1 when the temperature increased to 100 ºC. This indicated that the conformation (**1a**) can transform into the conformation (**1b**) at higher temperatures (Figures 3 and S9).

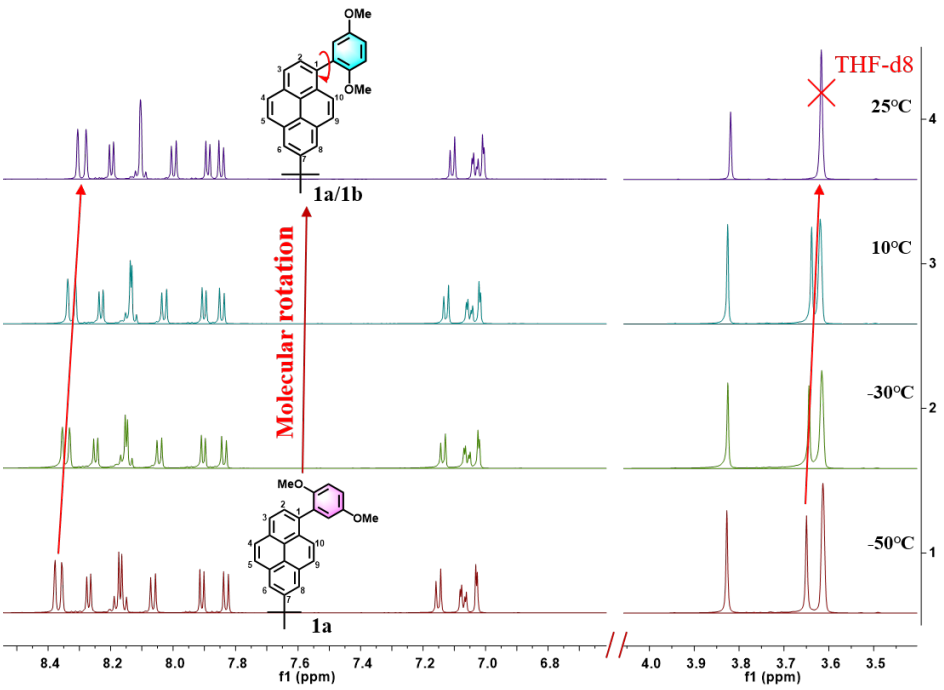

Figure 3. Variable-temperature ^{1}H NMR spectrum (600 MHz, 293 K, * THF-d8) of pyrene-based **1**.

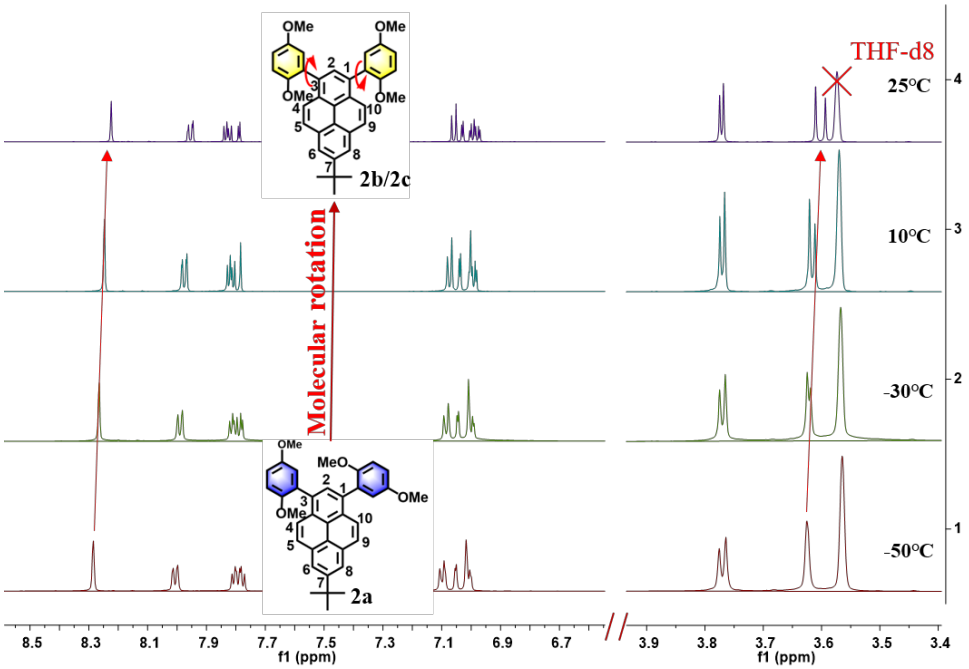

Figure 4. Variable-temperature ^{1}H NMR spectrum (600 MHz, 293 K, * THF-d8) of pyrene derivative **2**.

Similarly, the OMe group in compound **2** exhibits three single proton peaks at 3.63, 3.61 and 3.59 ppm with an integration ratio of 1:1:2, which indicates that there is one conformer at -50 ºC (Figure 4). Interestingly, the proton peak at 3.63 ppm has split into two peaks at 3.61 and 3.59 ppm, while the proton peak at *ca*. 3.77 ppm did not change as the temperature increased from -50 ºC to 25 ºC, indicating that the conformer of **2** has changed from conformation (**2a**) to conformation (**2b**), According to the ^{1}H NMR spectra of compound **2**, the mole ratio of conformations **2a** and **2b** is 6:4 (integral ratio). Moreover, as the temperature increased to 100 ºC, the overlapped proton singals for pyrene ring at 8.27, 8.06, 7.75, and 7.72 ppm became clearer, and the integral ratio of the proton peaks at 3.76 and 3.59 is 1:1. The result indicated that the molecular comformation (**2b**) could transfer to conformation (**2c**) (Figure S10). For compounds **3** and **4**, the proton peaks for the OMe group are in the range 3.55-3.80 ppm, and this becomes clearer as the temperature increases from -50 to 100 ºC (Figures S11, S12, S13, S14). It is thought that the compounds demonstrate various molecular conformations via molecular rotation around the C-C bond, and the dynamics products at low temperature can transfer to thermodynamic products at higher temperature. According to the DFT calculations, due to the low energy barrier (ΔE) between the conformers, the substituents group can rotate around the C-C bond, resulting in diverse molecular conformations. On the other hand, the sterically bulky 1,4-dimethoxylphenyl group can induce a stereoisomeric effect in this pyrene-based system, and the protons of each molecular conformation display a different chemical environment.

Photophysical Properties

The UV-vis absorption and emission spectra of these new pyrene-based compounds **1-4** were measured in dilute THF solution and are presented in Figure 5; the photophysical data are summarized in Table 1. These compounds exhibit quite similar absorption behaviour with strong absorption in the UV region (270-300 nm) and in the visible region (350-424 nm). The short-wavelength absorption is assigned to a π-π transition and the long-wavelength absorption belongs to a n-π* transition. As the number of substituents increased, the maximum long-wavelength absorption peak was red-shifted

from 344 to 378 nm following the order **1** < **2** < **3** < **4**. This can be ascribed to the expanding π-conjugated molecular frameworks. Moreover, compound **1** displays a large molar absorption coefficient (ε) of 39300 M^{-1} cm^{-1}, while the ε of compound **2** is 20500 M^{-1} cm^{-1}, indicating that the position-dependent substituent effect plays a significant role in influencing the electronic transition. [37]

Table 1. The photophysical properties of pyrene-based derivatives **1**-**4**.

Compd	$\lambda_{max,abs}$ (nm) (M^{-1} cm^{-1})	$\lambda_{max,em}$ (nm) *solns*[a]/*solns*[b]/*solid*[c]	FWHM (cm^{-1}) *solns*[a]/ *solid*[c]	Φf *solns*[a]/ *solid*[c]	τ (ns) *solns*[a]/ *solid*[c]	T_d
1	280(42500) 344(39300)	408/376, 395/409	62/37	0.25/0.07	8.63/20.62	304
2	285(24100) 356(20500)	399/379, 400/430	53/46	0.28/0.21	6.05/3.55	334
3	286(34500) 366(28100)	411/416/445	48/54	0.48/0.02	2.21/0.73	350
4	291(36200) 378(29300)	418/410,429/454	45/57	0.51/0.08	1.83/1.05	434

[a] Measured in THF solution at room temperature. [b] Measured in THF solution at 77K, [c] Measured as a solid.

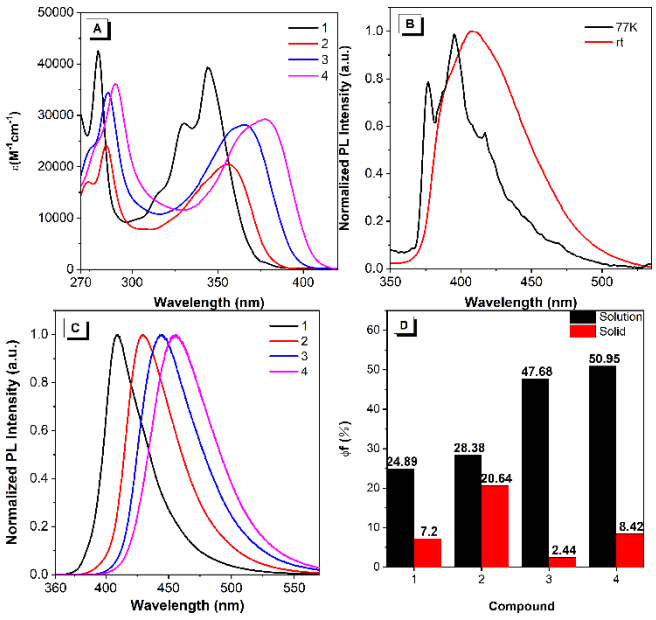

Figure 5. (A) UV-vis absorption and (B) Fluorescence spectra of compound **1** at 77K (black) and room temperature (red) in THF (~10^{-5}M); (C) Emission spectra of compounds **1**-**4** in the solid state; (D) quantum yields of compounds **1**-**4** in solution (black) and solid state (red).

Upon excitation, all compounds emit deep blue fluorescence with maximum emission peaks at 408 nm for **1**, 399 nm for **2**, 411 nm for **3** and 418 nm for **4** in THF solution, respectively. Compared to their solutions, these compounds exhibit a red-shifted emission of 409 nm for **1**, 430 nm for **2**, 445 nm for **3** and 454 nm for **4** in the solid state, respectively. Moreover, the full width at half maxima (FWHM) of the emission in solution tended to become narrower from 62 nm to 45 nm, which implied that the free molecular rotation induced a diversiform of molecular conformations and making the energy gap more complicated. In turn, this lead to a broadened emission band, while as the number of substituent groups increased, the steric effect of substituents could inhibit the molecular rotation in solution. In contrast, the FWHM of the emission became broader on moving from compound **1** (37 nm), through to compound **2** (46 nm), compound **3** (54 nm) and to compound **4** (57 nm). It is possible here that the molecular conformation has been fixed by weak intramolecular interactions, and more substituents could increase the numbers of molecular conformations, resulting in a broaden FWHM emission. Furthermore, the PL spectra of compounds **1**-**4** were measured at 77K, and are presented in Figures 5B and S24. Taking compound **1** as an example, looking at its optical behaviour at room temperature, compound **1** exhibits a narrower FWHM, and unresolved photoluminescence with a maximum emission 395 nm with a shoulder peak at 376 nm, indicating that compound **1** prefers to adopt a kinetic molecular conformation. Compound **2** exhibits similar emission behaviour as compound **1** at 77K, while the disordered rotation of terminal group against the pyrene ring, compounds **3** and **4** demonstrate similar emission properties as seen at room temperature. In addition, the fluorescence quantum yield is in range 0.25 to 0.51 in solution, but was almost quenched 1-24-fold in the solid state. Meanwhile, the fluorescence lifetime decreased in the solid state compared to in solution, which may be due to the closer molecular packing in the solid state. Viscosity-dependent PL experiments for compound **1-4** were carried out in mixtures of DMSO/ glycerol with different fractions ($f_{Vglycerol:VDMSO}$). As shown in Figure S26, the emission gradually decreased and the FWHM became wider as the fraction of glycerol increased, which suggested that the molecular conformation

is under an uniform system via a free molecular rotation in DMSO solution, and the molecular conformation could be fixed by employing a high viscosity solvent.

Solvatochromic effects

Generally, pyrene is very sensitive to changes in its microenvironment, and may act as an electron-donating group or an electron-withdrawing group depending on the molecular structure. Moreover, substituents introduced at the 1-, 3-, 6- and 8-positions of pyrene can increase the electronic communication with each other. To investigate the effect of polar solvents on the optical behaviour, the photophysical properties of compounds **1**-**4** were measured in six organic solvents (such as cyclohexane (Cy), tetrahydrofuran (THF), 1,4-dioxane, *N*,*N*-dimethylformamide (DMF), acetonitrile (ACN) and dimethyl sulfoxide (DMSO)). As shown in Figures 6 and S23, as the solvent polarity increases from Cy to DMSO, the UV-vis spectra slightly changed for **1**-**4**, while the emission shows different properties. Compound **1** exhibits a large red-shifted emission from 377 nm in non-polar solvent (cyclohexane) moving to 454 nm in polar solvent (DMSO). On increasing the number of substituents, the compounds display a small red-shifted emission, namely 149253 cm^{-1} (64 nm) for **1**, 172413 cm^{-1} (58 nm) for **2**, 277778 cm^{-1} (36 nm) for **3** and 714285 cm^{-1} (14 nm) for **4**, respectively. This may mean that the electronic distribution becomes more balanced between the substituents and the pyrene core, which is consisting with the DFT calculations.

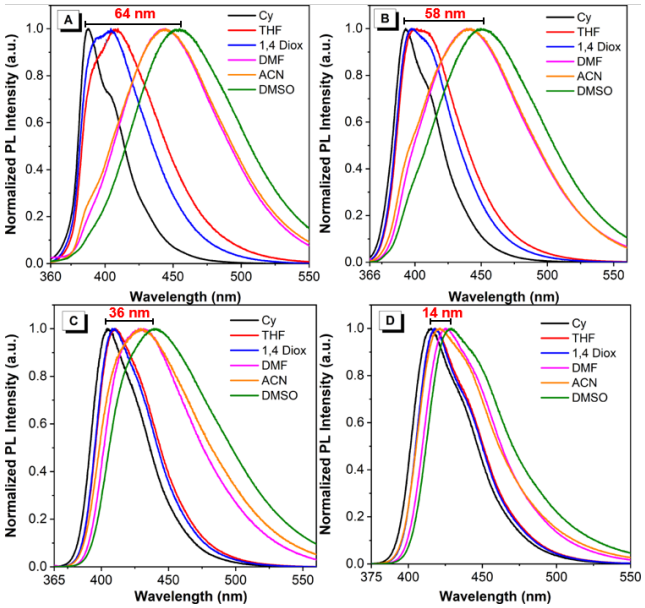

Figure 6. Solvent polarity-dependant fluorescence spectra measurement (A) compound **1**, (B) compound **2,** (C) compound **3** and (D) compound **4**, respectively.

Conclusions

In summary, this article presents four new pyrene-based blue emitters with various molecular conformations, due to the presence of stereoscopic OMe groups located at the 1-, 3-, 6- and 8-positions. Moreover, according to the DFT calculations, due to the relatively low potential-energy gap, the molecular skeleton can freely rotate around the single C-C bond, leading to different molecular conformations, which has been further confirmed by variable-temperature ^{1}H NMR spectroscopy. On the other hand, the various molecular conformations can cause broadened emission bands. This fundamental research was performed to not only to understand the molecular rotation, but also will be helpful for developing new high colour purity and narrow FWHM of organic luminescence materials.

CRediT authorship contribution statement

Xinyi Song: Investigation, resources and visualization. Hongxi Guo: Investigation. Shuning Yu: Investigation. Carl Redshaw: Writing - review &

editing. Qilong Zhang: Formal analysis. Ruquan Ye: Writing - review & editing. Xing Feng: Data curation, conceptualization, Writing-original draft, supervision, project administration.

Declaration of competing interest

There are no conflicts to declare.

Acknowledgements

This work was supported by the National Natural Science Foundation of China (21975054), Natural Science Foundation of Guangdong Province of China (2019A1515010925), Guangdong Provincial Key Laboratory of Information Photonics Technology (2020B121201011), "One Hundred Talents Program" of the Guangdong University of Technology (GDUT) (1108-220413205), the Open Fund of Guangdong Provincial Key Laboratory of Luminescence from Molecular Aggregates, Guangzhou 510640, China (South China University of Technology) (2019B030301003), Science and Technology Planning Project of Hunan Province (2018TP1017), CR thanks the University of Hull for support.

References

[1] Yang Z, Mao Z, Xie Z, Zhang Y, Liu S, Zhao J, Xu J, Chi Z, Aldred MP. Recent advances in organic thermally activated delayed fluorescence materials. Chem Soc Rev 2017;46(3):915-1016.

[2] Belmonte-Vázquez JL, Amador-Sánchez YA, Rodríguez-Cortés LA, Rodríguez-Molina B. Dual-State Emission (DSE) in Organic Fluorophores: Design and Applications. Chem Mater 2021;33(18):7160-7184.

[3] Xu Y, Xu R, Wang Z, Zhou Y, Shen Q, Ji W, Dang D, Meng L, Tang BZ. Recent advances in luminescent materials for super-resolution imaging via stimulated emission depletion nanoscopy. Chem Soc Rev 2021;50(1):667-690.

[4] Nie H, Wei Z, Ni XL, Liu Y. Assembly and Applications of Macrocyclic-Confinement-Derived Supramolecular Organic Luminescent Emissions from Cucurbiturils. Chem Rev 2022;122(9):9032-9077.

[5] Mu Y, Yang Z, Chen J, Yang Z, Li W, Tan X, Mao Z, Yu T, Zhao J, Zheng S, Liu S, Zhang Y, Chi Z, Xu J, Aldred MP. Mechano-induced persistent room-

temperature phosphorescence from purely organic molecules. Chem Sci 2018;9(15):3782-3787.

[6] Wang X, Wang L, Mao X, Wang Q, Mu Z, An L, Zhang W, Feng X, Redshaw C, Cao C, Qin A, Tang BZ. Pyrene-based aggregation-induced emission luminogens (AIEgens) with less colour migration for anti-counterfeiting applications. J MaterChem C 2021;9(37):12828-12838.

[7] Zeng J, Wang X, Song X, Liu Y, Liao B, Bai J, Redshaw C, Chen Q, Feng X. Steric influences on the photophysical properties of pyrene-based derivatives; mechanochromism and their pH-responsive ability. Dyes Pigm 2022;200:110123.

[8] Wang X, Zhang J, Mao X, Liu Y, Li R, Bai J, Zhang J, Redshaw C, Feng X, Tang BZ. Intermolecular Hydrogen-Bond-Assisted Solid-State Dual-Emission Molecules with Mechanical Force-Induced Enhanced Emission. J Org Chem 2022;87(13):8503-8514.

[9] Guell-Grau P, Escudero P, Perdikos FG, Lopez-Barbera JF, Pascual-Izarra C, Villa R, Nogues J, Sepulveda B, Alvarez M. Mechanochromic Detection for Soft Opto-Magnetic Actuators. ACS Appl Mater Interfaces 2021;13(40):47871-47881.

[10] Inci E, Topcu G, Guner T, Demirkurt M, Demir MM. Recent developments of colorimetric mechanical sensors based on polymer composites. J Mater Chem C 2020;8(35):12036-12053.

[11] Feng X, Zhang J, Hu Z, Wang Q, Islam MM, Ni J-S, Elsegood MRJ, Lam JWY, Zhou E, Tang BZ. Pyrene-based aggregation-induced emission luminogens (AIEgen): structure correlated with particle size distribution and mechanochromism. J Mater Chem C 2019;7(23):6932-6940.

[12] Qin L, Gu W, Wei J, Yu Y. Piecewise Phototuning of Self-Organized Helical Superstructures. Adv Mater 2018;30(8):1704941.

[13] Qu K, Duan P, Wang JY, Zhang B, Zhang QC, Hong W, Chen ZN. Capturing the Rotation of One Molecular Crank by Single-Molecule Conductance. Nano Lett 2021;21(22):9729-9735.

[14] Liu S, Zhou X, Zhang H, Ou H, Lam JWY, Liu Y, Shi L, Ding D, Tang BZ. Molecular Motion in Aggregates: Manipulating TICT for Boosting Photothermal

Theranostics. J Am Chem Soc 2019;141(13):5359-5368.

[15] Filatov M, Olivucci M. Designing conical intersections for light-driven single molecule rotary motors: from precessional to axial motion. J Org Chem 2014;79(8):3587-3600.

[16] Liao P, Huang J, Yan Y, Tang BZ. Clusterization-triggered emission (CTE): one for all, all for one. Mater Chem Front 2021;5(18):6693-6717.

[17] Dickinson E, Allison SA, McCammon JA. Brownian dynamics with rotation–translation coupling. J Chem Soc, Faraday Trans 2 1985;81(4):591-601.

[18] Mei J, Leung NL, Kwok RT, Lam JW, Tang BZ. Aggregation-Induced Emission: Together We Shine, United We Soar! Chem Rev 2015;115(21):11718-11940.

[19] Ma S, Du S, Pan G, Dai S, Xu B, Tian W. Organic molecular aggregates: From aggregation structure to emission property. Aggregate 2021;2(4):e96.

[20] Peng Q, Shuai Z. Molecular mechanism of aggregation-induced emission. Aggregate 2021;2(5):e91.

[21] Luo J, Xie Z, Lam JW, Cheng L, Chen H, Qiu C, Kwok HS, Zhan X, Liu Y, Zhu D, Tang BZ. Aggregation-induced emission of 1-methyl-1,2,3,4,5-pentaphenylsilole. Chem Commun 2001(18):1740-1741.

[22] Yan D, Wu Q, Wang D, Tang BZ. Innovative Synthetic Procedures for Luminogens Showing Aggregation-Induced Emission. Angew Chem Int Ed 2021;60(29):15724-15742.

[23] Pescitelli G, Di Bari L, Berova N. Conformational aspects in the studies of organic compounds by electronic circular dichroism. Chem Soc Rev 2011;40(9):4603-4625.

[24] Islam MM, Hu Z, Wang Q, Redshaw C, Feng X. Pyrene-based aggregation-induced emission luminogens and their applications. Mater Chem Front 2019;3(5):762-781.

[25] Wang X, Zhang C, Zeng J, Mao X, Redshaw C, Niu G, Yu X, Feng X. One-Pot Synthesis of Pyreno[2,1-b]furan Molecules with Two-Photon Absorption Properties. J Org Chem 2022, DOI: 10.1021/acs.joc.2c01303.

[26] Jiang W, Shen Y, Ge Y, Zhou C, Wen Y, Liu H, Liu H, Zhang S, Lu P, Yang B. A

single-molecule conformation modulating crystalline polymorph of a physical π–π pyrene dimer: blue and green emissions of a pyrene excimer. J Mater Chem C 2020;8(10):3367-3373.

[27] Oh H, Lee C, Lee S. Efficient blue organic light-emitting diodes using newly-developed pyrene-based electron transport materials. Org Electron 2009;10(1):163-169.

[28] Figueira-Duarte TM, Mullen K. Pyrene-based materials for organic electronics. Chem Rev 2011;111(11):7260-7314.

[29] Feng X, Hu JY, Redshaw C, Yamato T. Functionalization of Pyrene To Prepare Luminescent Materials-Typical Examples of Synthetic Methodology. Chem Eur J 2016;22(34):11898-11916.

[30] Feng X, Hu JY, Yi L, Seto N, Tao Z, Redshaw C, Elsegood MRJ, Yamato T. Pyrene-Based Y-shaped Solid-State Blue Emitters: Synthesis, Characterization, and Photoluminescence. Chem Asian J 2012;7(12):2854-2863.

[31] Mao XY, Xie FL, Wang XH, Wang QS, Qiu ZP, Elsegood MRJ, Bai J, Feng X, Redshaw C, Huo YP, Hu JY, Chen Q. New Quinoxaline-Based Blue Emitters: Molecular Structures, Aggregation-Induced Enhanced Emission Characteristics and OLED Application. Chin J Chem 2021;39(8):2154-2162.

[32] SAINT and APEX 2. Software for CCD diffractometers. 2015.

[33] Sheldrick GM. SHELXT - integrated space-group and crystal-structure determination. Acta Crystallogr A Found Adv 2015;71(Pt 1):3-8.

[34] Sheldrick GM. A short history of SHELX. Acta Crystallogr A 2008;64(Pt 1):112-122.

[35] Kung Y-C, Hsiao S-H. Fluorescent and electrochromic polyamides with pyrenylamine chromophore. J Mater Chem 2010;20(26):5481-5492.

[36] Janiak C. A critical account on π–π stacking in metal complexes with aromatic nitrogen-containing ligands†. Journal of the Chemical Society, Dalton Trans 2000(21):3885-96.

[37] Feng X, Hu J-Y, Tomiyasu H, Tao Z, Redshaw C, Elsegood MRJ, Horsburgh L,

Teat SJ, Wei X-F, Yamato T. Iron(iii) bromide catalyzed bromination of 2-tert-butylpyrene and corresponding position-dependent aryl-functionalized pyrene derivatives. RSC Adv 2015;5(12):8835-8848.